Journal of the Physical Society of Japan
Vol. 69, No. 7, July, 2000, pp. 2175–2181

Contact between Carbon Nanotube and Metallic Electrode

Takeshi NAKANISHI* and Tsuneya ANDO[1]

Institute of Physical and Chemical Research (RIKEN)
2–1 Hirosawa, Wako-shi, Saitama 351-0198

[1] *Institute for Solid State Physics, University of Tokyo*
5–1–5 Kashiwanoha, Kashiwa, Chiba 277-8581

(Received February 15, 2000)

Effects of a contact between a carbon nanotube and metallic electrode are studied in a tight-binding model. A model of dirty contact is introduced and discussed for electrode weakly coupled to a carbon nanotube. Measurements of a perfect transmission in two-terminal measurement may be possible by the using of the contact with both weak coupling and large area.

KEYWORDS: graphite, carbon nanotube, fullerene tube, contact resistance, recursive Green's function technique

§1. Introduction

Carbon nanotubes (CN's) are a new quantum wire consisting of rolled graphite sheets.[1)] They possess unique electronic properties due to their small diameter and intriguing lattice structure of a two-dimensional graphite. The purpose of this paper is to study a contact between an electrode and a metallic single-wall CN.

Transport properties of CN's are interesting because of their unique topological structure. There have been some reports on experimental study of transport in CN bundles connected at both ends to two gold pads.[2,3)] The magnetotransport of a single multi-wall nanotube was measured using tungsten or gold wires as an electrode.[4–7)] A single-wall CN was synthesized,[8,9)] and its transport was measured. Experiments showed large charging effects presumably due to nonideal contacts.[10–14)] By using liquid metal as a contact, a quantized conductance was observed in a multi-wall nanotube,[15)] but the quantized value turned out to be a half of the ideal value.

Various theoretical calculations were made on transport properties of CN. Tunneling probabilities of a finite-length CN[16)] and a connection of different CN's[17–23)] were calculated. The conductivity was calculated also in a constant-relaxation-time approximation in the absence of a magnetic field.[24)] The magnetoconductivity was calculated using the Boltzmann transport equation[25)] and in a transmission approach[26)] for a model of short-range scatterers. The results were shown to have a close connection with transport in a two-dimensional graphite sheet.[27)]

Effects of impurity scattering in CN's were studied and the complete absence of back scattering was proved rigorously except for scatterers having a potential range smaller than the lattice constant.[28)] This intriguing fact was related to Berry's phase acquired by a rotation in the wave vector space in the system described by a $\boldsymbol{k}\cdot\boldsymbol{p}$ Hamiltonian[29)] which is the same as Weyl's equation for a neutrino.[30)] The conductance was calculated in a tight-binding model by varying the strength of the potential.[31,32)]

Effects of scattering by a short-range and huge potential were studied in CN's in the presence and absence of a magnetic field.[19,33–37)] The conductance was shown to be quantized into zero, one, and two times of the conductance quantum $e^2/\pi\hbar$ depending on the type of the vacancy.

For the observation of such intriguing transport properties of CN realization of low contact resistance is absolutely necessary. Theoretically, such contact problems are quite interesting and are currently the subject of intensive study. For example, the transmission probability between a single-wall CN and a jellium metal was discussed[38)] and explicitly calculated.[39)] A coupling of CN with a copper chain was discussed using pseudopotential[40)] and that with a metal in a jellium model.[41)]

In this paper, the contact resistance between a metallic electrode and CN is studied in a model of a dirty metallic contact. In §2, a model of the contact is introduced and the method of the calculation is described. Results are presented in §3 and discussed in §4. A summary and conclusion are given in §5.

§2. Model of Contact and Methods

We consider a semi-infinite armchair nanotube with circumference $L=\sqrt{3}aM/2$ as shown in Fig. 1, where M is an integer and a is the lattice constant. A set of carbon atoms in the circumference direction will be called a cell and each cell is specified by an integer n starting with $n=1$ at the left end. We attach ideal leads to carbon atoms lying close to the left edge and calculate the conductance between the leads and CN. The conductance is proportional to the transmission probability

* Present address: Department of Applied Physics and DIMES, Delft University of Technology, Lorentzweg 1, 2628 CJ Delft, The Netherlands

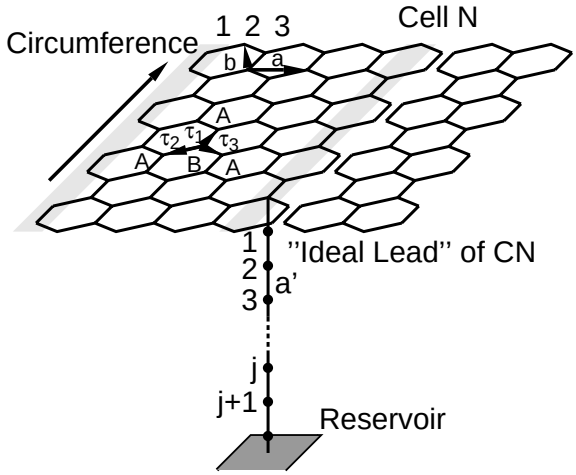

Fig. 1 Schematic illustration of the lattice structure of armchair CN and ideal leads. Only some part of CN is shown in the circumference direction. The cells $n=1$ and N are with shadow and the cell with $n=N+1$ is connected to an "ideal lead" of CN. Carbon atoms in cells $n=1$ to N are connected to a reservoir through an ideal lead characterized by the transfer integral t and lattice constant a'. The primitive translation vectors of the two-dimensional graphite are given by $\boldsymbol{a}$ and $\boldsymbol{b}$ and the lattice constant is $a=|\boldsymbol{a}|$. A unit cell contains two carbon atoms called A and B, which are connected by vectors $\vec{\tau}_1$, $\vec{\tau}_2$, and $\vec{\tau}_3$.

from leads to the tube region infinitely away according to Landauer's formula.[42)]

Consider first the case that a single ideal lead connected to a single carbon atom at a B site of a cell $n=N$. The equation of motion of the ideal lead consisting of a one-dimensional lattice is written by

$$\varepsilon C_j + tC_{j+1} + tC_{j-1} = 0, \tag{2.1}$$

where ε is the energy, C_j describes the amplitudes of site j, and t is the transfer integral between nearest neighbor atoms ($t>0$). An end of the ideal lead is connected to a carbon atom chosen as $j=0$ and the other end infinitely away is connected to a reservoir. For simplicity, the energy of each atom is chosen to be same as that of a carbon, i.e., the band center of CN at the Fermi level. At $j=0$,

$$\varepsilon C_0 + \gamma_0 \sum_{i=1}^{3} C_{\vec{\tau}_i} = -tC_1, \tag{2.2}$$

where γ_0 is the transfer integral between three nearest-neighbor A and B sites, which are connected by vectors $\vec{\tau}_1$, $\vec{\tau}_2$, and $\vec{\tau}_3$ in CN as shown in Fig. 1. If the ideal lead is connected to an A site in CN's, $\vec{\tau}_i$ are replaced by $-\vec{\tau}_i$ in eq. (2.2).

In the ideal lead, we have

$$\varepsilon = -2t\cos(k'a'), \tag{2.3}$$

where a' is the lattice constant and k' is the wave vector, and the corresponding velocity is given by

$$v(k') = \frac{2ta'}{\hbar}\sin(k'a'). \tag{2.4}$$

First, we have to separate C_0 into in-coming and out-going solutions in the ideal lead. We shall write

$$C_0 = C_0^{(-)} + C_0^{(+)}, \tag{2.5}$$

where $-$ and $+$ denote in-coming and out-going components, respectively. Then, we have

$$\begin{aligned} C_1 &= \exp(-\mathrm{i}k'a')C_0^{(-)} + \exp(+\mathrm{i}k'a')C_0^{(+)} \\ &= \exp(-\mathrm{i}k'a')C_0^{(-)} + \exp(+\mathrm{i}k'a')[C_0 - C_0^{(-)}], \end{aligned} \tag{2.6}$$

where $k'>0$ for a given ε ($-2t \le \varepsilon \le +2t$). The substitution of this into eq. (2.2) gives

$$(\varepsilon-\Sigma)C_0 + \gamma_0 \sum_{i=1}^{3} C_{\vec{\tau}_i} = \frac{\mathrm{i}\hbar v(k')}{a'} C_0^{(-)}, \tag{2.7}$$

with

$$\Sigma = -t\exp(\mathrm{i}k'a'). \tag{2.8}$$

The term Σ can be viewed as a self-energy arising from the interaction of CN with the ideal lead and $t=|\Sigma|$ is the parameter describing the coupling strength between the electrode and CN.

An "ideal lead" consisting of an armchair CN with infinite length is attached starting with the cell at $n=N+1$. The condition that only right-going (out-going) waves can exist at $n=N+1$ is included in a usual manner[43)] and gives a self-energy term similar to Σ in eq. (2.7) at the cell $n=N+1$. The Green's function can be calculated by inverting such effective Hamiltonian for $n=1$ to $N+1$ including such self-energy terms.

The transmission coefficient for a wave injected from the ideal lead attached to a carbon atom to the ideal lead of an armchair CN infinitely long can be calculated using this Green's function. In fact, we first calculate the amplitude at the cell $n=N+1$ using the Green's function and treating the right hand side of eq. (2.7) as a source term. Then, the resulting amplitude at $n=N+1$ is separated into traveling waves at the K and K' points. In the source term at a site $j=0$ in the cell $n=N$, we should put $C_0^{(-)} = 1/\sqrt{|v(k')|}$ corresponding to a unit flux of the in-coming wave and have

$$(\varepsilon-\Sigma)C_0 + \gamma_0 \sum_{i=1}^{3} C_{\vec{\tau}_i} = \frac{\mathrm{i}\hbar\sqrt{|v(k')|}}{a'}. \tag{2.9}$$

The traveling waves of CN at $n=N+1$ should also be normalized such that they carry a unit flux.

Armchair nanotubes are always metallic and the conduction and valence bands have a linear dispersion and cross the Fermi level at the K and K' points corresponding to $K=2\pi/3a$ and $K'=-2\pi/3a$, respectively. In fact, we have $\varepsilon(k)=\gamma(k-K)$ for $k\sim K$ and $\varepsilon(k)=\gamma(k-K')$ for $k\sim K'$, where $\gamma=\sqrt{3}\gamma_0 a/2$ and k is the wave vector in CN along the axis direction. Therefore, in the nanotube infinitely away from the ideal lead there are two traveling modes associated with the K and K' point.

It is straightforward to extend the calculation to the case that ideal leads are connected to many carbon atoms in CN as long as leads attached to different carbon atoms are independent of each other. In this case N should be chosen such that ideal leads are connected to atoms in cells with $n\le N$ but not in cells with $n>N$. The

conductance is given by

$$G = \frac{e^2}{\pi\hbar}\sum_{\nu}\left(|t_{K\nu}|^2+|t_{K'\nu}|^2\right), \tag{2.10}$$

where ν specifies a carbon atom to which an ideal lead is attached and $t_{K\nu}$ and $t_{K'\nu}$ represent transmission from ν to the K and K' states in the ideal lead of CN. When a contact metal is not ideal, some carbon atoms are strongly coupled to electrode and others are weakly coupled due to randomness present in the contact region. Such disorder effects can be studied by varying the transfer integral t of ideal leads among different leads. In this case the effective coupling is characterized by the average transfer $t_{\rm av}$ and its width δt of the distribution.

We introduce time τ_ϕ during which an electron stays on a carbon atom in the contact region without going into ideal leads

$$\tau_\phi = \frac{\hbar}{|\mathrm{Im}\,\Sigma|}, \tag{2.11}$$

where Σ is the self-energy defined in eq. (2.8). By multiplying the velocity $\gamma/\hbar$ in CN, the corresponding length l_ϕ is defined by

$$l_\phi = \frac{\gamma\tau_\phi}{\hbar}, \tag{2.12}$$

where t should be replaced by $t_{\rm av}$ in the presence of randomness. This "phase coherence" length corresponds to the length of the nanotube covered by an electron before going into ideal leads when ideal leads are attached to all carbon atoms. The situation is analogous to systems in the presence of inelastic scattering introduced by Büttiker[44] and used for the study of the voltage distribution in the quantum Hall effect.[45]

So far we have assumed that the transfer integral t' between a carbon atom and a metal atom of the ideal lead is same as the transfer integral t between neighboring metal atoms. It is straightforward to extend the above discussion to the case $t' \neq t$ as discussed in Appendix A. The result shows that t in Σ given by eq. (2.8) and in $v(k')$ in eq. (2.9) should simply be replaced by t'^2/t, i.e., that the transmission coefficient becomes a function of t'^2/t and k'. For $\varepsilon = 0$, we have $k'a = \pi/2$ independent of t and t', showing that the transmission coefficient is obtained from that for $t'=t$ by the replacement $t \to t'^2/t$. For nonzero ε, the transmission coefficient becomes dependent on individual values of t and t' because k' depends on t through eq. (2.3). However, such dependence is negligible as long as $|\varepsilon|/\gamma_0 \ll 1$, which can be demonstrated both analytically and numerically.

§3. Numerical Results

3.1 Single Lead

In actual numerical calculations, carbon atoms are divided into the cells $n = 1, \ldots, N$ as mentioned above and Green's functions are calculated in terms of recursive Green's function technique[43] as in previous works.[22,31] We choose $\varepsilon = 0$ and $L = 50\sqrt{3}a$ in the following.

Figure 2 shows the calculated conductance between CN and a single ideal lead connected to a carbon atom. The probability of an electron to be transmitted into the K channel is always same as that into the K' channel although not shown explicitly.

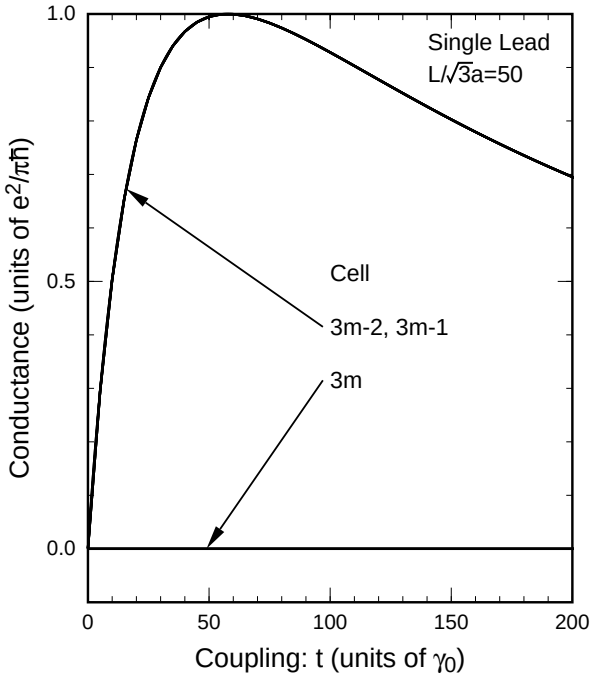

Fig. 2 Calculated conductance versus coupling strength t for CN with circumference $L/a = 50\sqrt{3}$, in which a single ideal lead is connected to a carbon atom on a specified cell n. The conductance for $n = 3m+1$ and that for $n = 3m+2$ are identical and that for $n = 3m$ vanishes, where m is an integer.

When the lead is attached to a carbon atom in cells $n = 3m-1$ or $3m-2$ with an integer m, the conductance increases linearly with the increase of coupling strength t, reaches a perfect transmission at a certain value of t, and then decreases. For small t the conductance increases with t, because the coupling between CN and the electrode becomes stronger. For large t, due to strong coupling an electron is reflected back to the ideal lead before being transmitted into the nanotube and as a result the conductance decreases with t. The value of t/γ_0 at the maximum conductance is $\sim$ 60 and is unrealistically large [calculations for other values of L show that $t/\gamma_0 \sim L/a$ at the maximum].

For the case $n = 3m$, on the other hand, we have a perfect reflection. This singular behavior is caused by interference of right-going and left-going waves in the presence of the hard wall at the left end of CN. In fact, because the Bloch phase of the wave functions at K and K' points changes as a function of n with period 3, the wave function which vanishes at $n = 0$ vanishes always at $n = 3m$. As a result, the ideal lead cannot couple with traveling modes in the nanotube when $n = 3m$.

3.2 Many Leads

Consider next the case that ideal leads with same t ($\delta t = 0$) are connected to all carbon atoms in several cells ($n = 1, \cdots, N$) of CN including the left end. Figure 3 shows the calculated conductance as a function of t for several values of N. The dependence on t is qualitatively same as that in the case of a single ideal lead, i.e., the conductance increases with t for small t, takes a maximum, and then starts to decrease. The value of

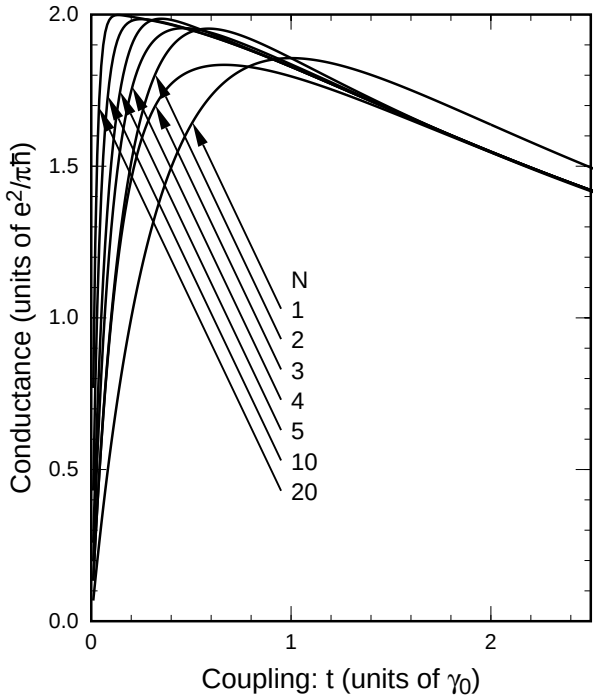

Fig. 3 Calculated conductance of CN with $L/a = 50\sqrt{3}$ as a function of the coupling t for several values of N.

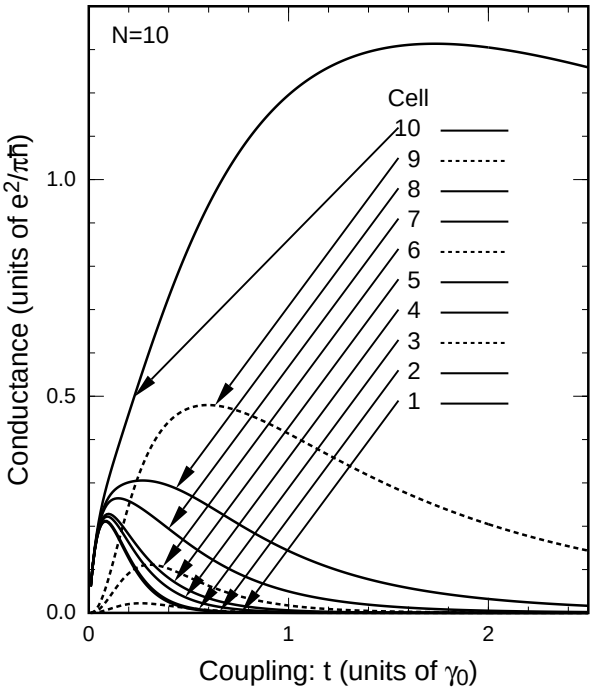

Fig. 4 Contributions to the conductance injected from ideal leads on each cell for $N = 10$. For cells with $n = 3m$ they are shown by dotted lines and for the others by solid lines. The corresponding conductance is given by the sum and is shown in Fig. 3.

t corresponding to the maximum conductance is much smaller than that of a single ideal lead and becomes smaller with the increase of the length of the region connected to ideal leads.

For $N=1$, in particular, where only the left end cell is connecting to ideal leads, the conductance G takes a maximum at $t/\gamma_0 = 1$. In this case the conductance can be calculated analytically as

$$G = \frac{e^2}{\pi\hbar} 4\sqrt{3}\Big(\frac{\gamma_0}{t} + \frac{t}{\gamma_0} + \sqrt{3}\Big)^{-1}, \tag{3.1}$$

although its derivation will not be discussed. It is interesting that this conductance has a symmetry $G(t/\gamma_0) = G(\gamma_0/t)$.

Figure 4 shows the contributions to the conductance injected from ideal leads on a specified cell for $N = 10$. For small $t/\gamma_0 \ll \sqrt{3}/N$, where $l_\phi \gg Na/2$, all cells with $n = 3m-1$ and $n = 3m-2$ equally contribute to the conductance and their contribution is proportional to t, whereas the contributions of cells with $n = 3m$ are proportional to t^2 and much smaller. This behavior corresponds to the main feature of the results for a single lead shown in Fig. 2. In fact, for a small t the probability for an electron to be scattered into other ideal leads is proportional to t^2 and can be neglected.

With the further increase of t, each contribution to the conductance takes a maximum and then decreases. For large t, the contribution to the conductance is larger for a cell with large n, i.e., away from the left end, and becomes negligibly small for $n \ll N$. The reason is that an electron transmitted into the tube from a lead in a cell close to the left end is almost always scattered into other leads before being going into the region of the nanotube without leads. Figure 4 shows that for $t/\gamma_0 \gtrsim 2$ the contributions of two cells $n = N$ and $N-1$ are dominant and other contributions are much smaller. This is the reason that the conductance is independent of N for $t/\gamma_0 \gtrsim 2$ for $N \geq 2$.

Figure 3 shows that the conductance exhibits an oscillatory dependence on N. The oscillation can be seen clearly in Fig. 5 where the dependence on N is shown for several values of t/γ_0. For sufficiently small values of t/γ_0 and for $Na/2 \lesssim l_\phi$ the conductance remains same for $N = 3m-1$ and $N = 3m$ with an integer m because the cell $n = 3m$ does not contribute to the conductance as mentioned above. For other values of t/γ_0, the conductance has a small dip at $N = 3m$ presumably because the cell $n = 3m$ contributes more to a drain for electrons injected from other leads rather than to an injection source. This oscillation does not disappear until the condition $Na/2 \gg l_\phi$ is satisfied.

Figure 6 shows calculated conductance as a function of t/γ_0 for large N. In the limit $N \to \infty$ the conductance comes up to the ideal value $G = 2e^2/\pi\hbar$ at $t/\gamma_0 = 0$ and decreases with the increase of t/γ_0 in proportion to $(t/\gamma_0)^2$. This reduction from the ideal value for nonzero t/γ_0 is due to reflection of the electron wave at the 'junction' between the nanotube with attached leads and the ideal nanotube lead. In fact, a small self-energy $\Sigma \propto t$ is present in carbon atoms in cells $n \leq N$ and not in $n \geq N+1$, leading to a small reflection at $n = N+1$ whose probability is proportional to $(|\Sigma|/\gamma_0)^2$. The results show clearly that a weak coupling between contacts and CN and a sufficiently large contact area are appropriate conditions for ideal electrodes, i.e., ideal for the observation of the conductance of a nanotube itself without any contact resistance.

3.3 Disorder Effects

It is expected that the average coupling $t_{\rm av}$ deter-

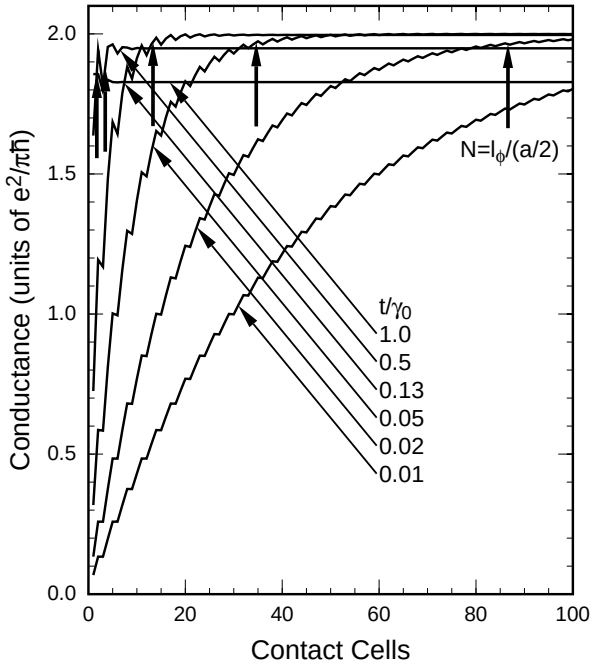

Fig. 5 Calculated conductance as a function of contact cells N for $t/\gamma_0 = 0.01$, 0.02, 0.05, 0.13, 0.4, and 1.0. The corresponding "phase coherence" lengths are $l_\phi/(a/2) = 170$, 87, 35, 13, 4.3, and 1.7. The vertical arrows indicate $N = l_\phi/(a/2)$.

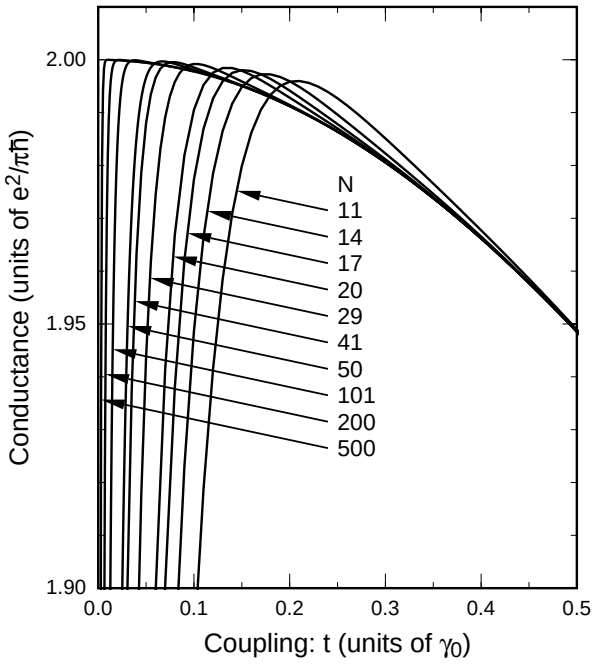

Fig. 6 Calculated conductance as a function of the coupling t for large N.

mines the conductance even in the presence of disorder when leads are attached to many cells. In order to see the validity of this expectation, we calculate the conductance for systems in which t is distributed uniformly in the region $t_{\rm av} - \delta t/2 < t < t_{\rm av} + \delta t/2$.

Figure 7 shows an example of the conductance averaged over 2500 different samples as a function of the number of the contact cells for $t_{\rm av}/\gamma_0 = 0.13$ and $\delta t = 2t_{\rm av} = 0.26$. The results for $L/\sqrt{3}a = 50$ and 25 are shown. The averaged conductance is identical for two

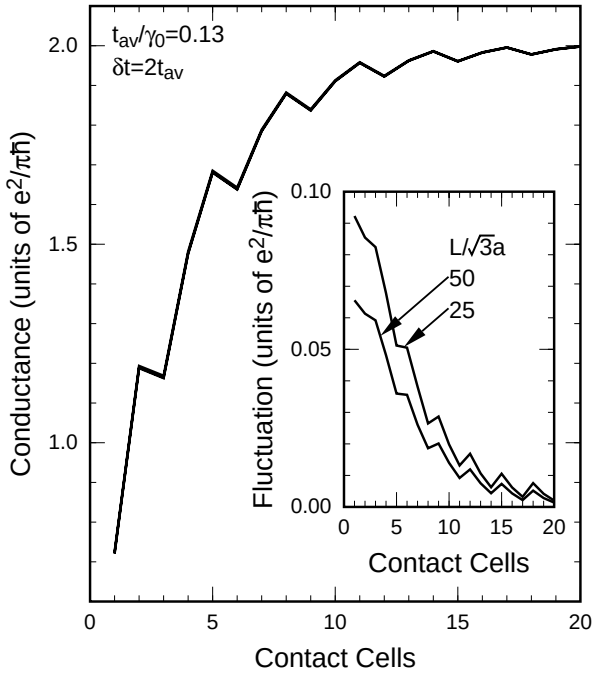

Fig. 7 The conductance averaged over 2500 different samples with $t_{\rm av}/\gamma_0 = 0.13$ and $\delta t = 2t_{\rm av} = 0.26$ in CN with $L/\sqrt{3}a = 50$ and $L/\sqrt{3}a = 25$. We have $l_\phi/(a/2) = 13$ for $t/\gamma_0 = 0.13$. The inset shows the fluctuation of the conductance.

cases and agrees with the conductance shown in Fig. 5 in the absence of randomness for $t = t_{\rm av}$. The inset shows the fluctuation given by $\Delta G = \sqrt{\langle (G - \langle G \rangle)^2 \rangle}$, where $\langle \cdots \rangle$ denotes the sample average. It shows that the fluctuation decreases with L and N in proportion to $1/\sqrt{LN}$ for small N as is expected. For a sufficiently large N the fluctuation becomes much smaller because the conductance approaches the ideal value.

§4. Discussion

If we consider a contact of a nanotube and surrounding uniform and ideal jellium metal, the conservation of the wave-vector component parallel to the CN axis imposes a strong constriction for the injection of electrons from a metal to CN.[38,39] Further, the Fermi level in the metal should be same as that of CN. States satisfying the conservation of the wave vector are usually located on a closed circle on the Fermi sphere of the metal. Transmission and reflection of waves having such a wave vector determine a contact resistance between the metallic electrode and CN. An *ab initio* pseudopotential calculation of nanotubes in the presence of surrounding jellium metal was reported recently,[41] suggesting that there can be considerable asymmetry in the coupling between to bands crossing the Fermi level.

The present model corresponds to a completely opposite situation. The most crucial assumption of the model is that leads connected to different carbon atoms are completely independent of each other. Strictly speaking, this can be justified only when the phase coherence length in the metallic electrode is smaller than or of the same order as the lattice constant of CN. Even if such conditions are not completely satisfied, the model may describe essential features in the case that the electrode

consists of dirty metals without translational symmetry. In actual experiments, various different metals are used as electrodes including liquid metals. They are mostly dirty metals without translational symmetry.

When we use a known value of the Fermi velocity v_F, for example, we can determine the parameter t/γ_0 for each metal using eq. (2.4) at $\varepsilon=0$. In fact, we have $t/\gamma_0 \sim 0.762$ for Cu, 0.679 for Au, and 0.766 for Hg corresponding to $v_F=1.57$, 1.40, and 1.58 in units of 10^8 cm/s. In realistic cases the transfer integral t' between a carbon atom and a metal atom can be quite different form t and may be reduced considerably by randomness of the contact surface or mismatch of a lattice constant. As is discussed in Appendix A, the calculation can be extended easily to such a case and the result shows that the important coupling parameter t is replaced by t'^2/t which can be much smaller than t.

§5. Summary and Conclusion

We have studied the conductance between CN and a dirty metallic contact using the model in which a single ideal lead is attached to each carbon atom in the contact region. The result shows that the negligible contact resistance can be realized if we make the coupling between CN and the electrode sufficiently small, i.e., $t/\gamma_0 \ll 1$, and the contact area sufficiently large. For such contacts, fluctuations in the coupling strength due to randomness are not important because the effective coupling between CN and an electrode is essentially determined by an average over a large area.

Acknowledgments

This work was supported in part by Grant-in-Aid for Scientific Research from Ministry of Education, Science and Culture. One of us (T. N.) acknowledges the support of a fellowship from Special Postdoctoral Researches Program at RIKEN. Numerical calculations were performed in part on FACOM VPP500 in Supercomputer Center, Institute for Solid State Physics, University of Tokyo, and in Institute of Physical and Chemical Research.

Appendix A: Generalization

Let t' be the transfer integral between an ideal lead defined by eq. (2.1) and a carbon atom in CN. Then, the equations of motion become

$$\varepsilon C_0 + \gamma_0 \sum_{i=1}^{3} C_{\vec{\tau}_i} = -t' C_1, \tag{A1}$$

at $j=0$ and

$$\varepsilon C_1 + t' C_0 + t C_2 = 0, \tag{A2}$$

at $j=1$. They are given by eq. (2.1) for $j>1$. We separate C_1 into in-coming $C_1^{(-)}$ and out-going $C_1^{(+)}$ waves, i.e.,

$$C_1 = C_1^{(-)} + C_1^{(+)}. \tag{A3}$$

Then, we have

$$\begin{aligned} C_2 &= C_1^{(-)} \mathrm{e}^{-\mathrm{i}k'a'} + C_1^{(+)} \mathrm{e}^{\mathrm{i}k'a'} \\ &= C_1^{(-)} \mathrm{e}^{-\mathrm{i}k'a'} + [C_1 - C_1^{(-)}] \mathrm{e}^{\mathrm{i}k'a'}. \end{aligned} \tag{A4}$$

The substitution of this into eq. (A2) gives

$$C_1 = \frac{t'}{t} \mathrm{e}^{\mathrm{i}k'a'} C_0 - \mathrm{i} \frac{\hbar v(k')}{ta'} \mathrm{e}^{\mathrm{i}k'a'} C_1^{(-)}. \tag{A5}$$

Define

$$C_0^{(-)} = \mathrm{e}^{\mathrm{i}k'a'} C_1^{(-)}, \tag{A6}$$

and substitute the above into eq. (A1). Then, we have

$$(\varepsilon - \Sigma') C_0 + \gamma_0 \sum_{i=1}^{3} C_{\vec{\tau}_i} = \mathrm{i} \frac{\hbar t' v(k')}{ta'} C_0^{(-)}, \tag{A7}$$

where

$$\Sigma' = -\frac{t'^2}{t} \mathrm{e}^{\mathrm{i}k'a'}. \tag{A8}$$

This shows that the self-energy is obtained from eq. (2.8) by the replacement $t \to t'^2/t$.

In order to calculate the transmission coefficient for a wave injected from the ideal lead, we have to substitute $C_0^{(-)} = 1/\sqrt{|v(k')|}$ corresponding to a unit flux. Then, we have

$$(\varepsilon - \Sigma') C_0 + \gamma_0 \sum_{i=1}^{3} C_{\vec{\tau}_i} = \mathrm{i} \frac{\hbar \sqrt{|v'(k')|}}{a'}, \tag{A9}$$

where

$$v'(k') = \frac{2t'^2 a'}{\hbar t} \sin(k'a'). \tag{A10}$$

This shows clearly that the equation of motion at $j=0$ can be obtained from eq. (2.7) by the replacement $t \to t'^2/t$.

For $\varepsilon = 0$, we have $k'a = \pi/2$ independent of t and t', showing that the transmission coefficient is obtained from that for $t' = t$ by the replacement $t \to t'^2/t$. For nonzero ε, the transmission coefficient becomes dependent on individual values of t and t' because k' depends on ε and t explicitly [see eq. (2.3)]. However, as long as the condition $|\varepsilon|/\gamma_0 \ll 1$ is satisfied, the condition $|\varepsilon|/t \ll 1$ is fulfilled usually because $|t|$ and γ_0 are of the same order. In this case the explicit dependence on t and t' remains small and can be neglected. This can be shown analytically and can be confirmed also by direct numerical calculations

1) S. Iijima: Nature **354** (1991) 56.
2) S. N. Song, X. K. Wang, R. P. H. Chang, and J. B. Ketterson: Phys. Rev. Lett. **72** (1994) 697.
3) L. Langer, L. Stockman, J. P. Heremans, V. Bayot, C. H. Olk, C. Van Haesendonck, Y. Brunseraede, and J-P. Issi: J. Mater. Res. **9** (1994) 927.
4) L. Langer, V. Bayot, E. Grive, J. -P. Issi, J. P. Heremans, C. H. Olk, L. Stockman, C. Van Haesendonck, and Y. Brunseraede: Phys. Rev. Lett. **76** (1996) 479.
5) T. W. Ebbesen, H. J. Lezec, H. Hiura, J. W. Bennett, H. F. Ghaemi, and T. Thio: Nature **382** (1996) 54.
6) F. Katayama: Master thesis (Univ. Tokyo, 1996).
7) A. Fujiwara, K. Tomiyama, and H. Suematsu: Phys. Rev. B **60** (1999) 13492.
8) S. Iijima and T. Ichihashi: Nature **363** (1993) 603.
9) D. S. Bethune, C. H. Kiang, M. S. de Vries, G. Gorman, R. Savoy, J. Vazquez, and R. Beyers: Nature

363 (1993) 605.
10) S. J. Tans, M. H. Devoret, H. -J. Dai, A. Thess, R. E. Smalley, L. J. Geerligs, and C. Dekker: Nature **386** (1997) 474.
11) M. Bockrath, D. H. Cobden, P. L. McEuen, N. G. Chopra, A. Zettl, A. Thess, and R. E. Smalley: Science **275** (1997) 1922.
12) S. J. Tans, M. H. Devoret, R. J. A. Groeneveld, and C. Dekker: Nature **394** (1998) 761.
13) D. H. Cobden, M. Bockrath, P. L. McEuen, A. G. Rinzler, and R. E. Smalley: Phys. Rev. Lett. **81** (1998) 681.
14) A. Bezryadin, A. R. M. Verschueren, S. J. Tans, and C. Dekker: Phys. Rev. Lett. **80** (1998) 4036.
15) S. Frank, P. Poncharal, Z. L. Wang and W. A. de Heer: Science **280** (1998) 1744.
16) W. -D. Tian and S. Datta: Phys. Rev. B **49** (1994) 5097.
17) R. Saito, G. Dresselhaus, and M. S. Dresselhaus: Phys. Rev. B **53** (1996) 2044.
18) L. Chico, V. H. Crespi, L. X. Benedict, S. G. Louie, and M. L. Cohen: Phys. Rev. Lett. **76** (1996) 971.
19) L. Chico, L. X. Benedict, S. G. Louie, and M. L. Cohen: Phys. Rev. B **54** (1996) 2600.
20) R. Tamura and M. Tsukada: Solid State Commun. **101** (1997) 601.
21) R. Tamura and M. Tsukada: Phys. Rev. B **55** (1997) 4991.
22) T. Nakanishi and T. Ando: J. Phys. Soc. Jpn. **66** (1997) 2973.
23) H. Matsumura and T. Ando: J. Phys. Soc. Jpn. **67** (1998) 3542.
24) Y. Miyamoto, S. G. Louie, and M. L. Cohen: Phys. Rev. Lett. **76** (1996) 2121.
25) T. Seri and T. Ando: J. Phys. Soc. Jpn. **66** (1997) 169.
26) T. Ando and T. Seri: J. Phys. Soc. Jpn. **66** (1997) 3558.
27) N. H. Shon and T. Ando: J. Phys. Soc. Jpn. **67** (1998) 2421.
28) T. Ando and T. Nakanishi: J. Phys. Soc. Jpn. **67** (1998) 1704. There are some typographical errors in this paper. For example, $u_A(\mathbf{R}_A)$ and $u_B(\mathbf{R}_B)$ appearing in the right hand side of eq. (2.18) should be replaced by $\tilde{u}_A(\mathbf{R}_A)$ and $\tilde{u}_B(\mathbf{R}_B)$, respectively.
29) H. Ajiki and T. Ando: J. Phys. Soc. Jpn. **62** (1993) 1255.
30) T. Ando, T. Nakanishi, and R. Saito: J. Phys. Soc. Jpn. **67** (1998) 2857.
31) T. Nakanishi and T. Ando: J. Phys. Soc. Jpn. **68** (1999) 561.
32) T. Ando, T. Nakanishi and R. Saito: Microelectronic Engineering **47** (1999) 421.
33) M. Igami, T. Nakanishi and T. Ando: J. Phys. Soc. Jpn. **68** (1999) 716.
34) M. Igami, T. Nakanishi and T. Ando: Mol. Cryst. Liq. Cryst. (in press).
35) M. Igami, T. Nakanishi and T. Ando: J. Phys. Soc. Jpn. **68** (1999) 3146.
36) T. Nakanishi, M. Igami and T. Ando: Physica E (in press).
37) T. Ando, T. Nakanishi, and M. Igami: J. Phys. Soc. Jpn. **68** (1999) 3994.
38) J. Tersoff: Appl. Phys. Lett. **74** (1999) 2122.
39) M. P. Anantram, S. Datta, and Y. Xue: cond-mat/9907357.
40) K. Kong, S. Han, and J. Ihm: Phys. Rev. B **60** (1999) 6074.
41) H. J. Choi, J. Ihm, Y. -G. Yoon, and S. G. Louie: Phys. Rev. B **60** (1999) R14009.
42) R. Landauer: IBM J. Res. Dev. **1** (1957) 223; Philos. Mag. **21** (1970) 863.
43) T. Ando: Phys. Rev. B **44** (1991) 8017.
44) M. Büttiker: Phys. Rev. B **32** (1985) 1846; Phys. Rev. B **33** (1986) 3020; IBM J. Res. Develop. **32** (1988) 63.
45) T. Ando: Surf. Sci. **361/362** (1996) 270; Physica B **249-251** (1998) 84.